arXiv:1609.04326v1 [astro-ph.SR] 14 Sep 2016

Photometric Calibration of the [α/Fe] Element: I. Calibration with UBV Photometry

S. Karaali [1] • E. Yaz Gökçe [1] • S. Bilir [1]

Abstract We present the calibration of the [α/Fe] element in terms of the ultra-violet excess for 469 dwarf stars with $0.325 < (B-V)_0 \leq 0.775$ mag corresponding the spectral type range F0-K2. The star sample is separated into nine sub-samples with equal range in $(B-V)_0$ colour, $\Delta(B-V)_0 = 0.05$ mag, and a third degree polynomial is fitted to each dataset. Our calibrations provide [α/Fe] elements in the range [0.0, 0.4]. We applied the procedure to two sets of field stars and two sets of clusters. The mean and the corresponding standard deviation of the residuals for 43 field stars taken from the Hypatia catalogue are [α/Fe]=-0.090 and $\sigma = 0.102$ dex, while for the 39 ones taken from the same catalogue of stars used in the calibration are [α/Fe]=-0.009 and $\sigma = 0.079$ dex, respectively. We showed that the differences between the mean of the residuals and standard deviations for two sets of clusters ([α/Fe]=0.073 and $\sigma = 0.91$ dex; [α/Fe]=-0.012 and $\sigma = 0.053$ dex) originate from the $(B-V)_0$ and $(U-B)_0$ colour indices of the clusters which are taken from different sources. The differences between the original [α/Fe] elements and the estimated ones (the residuals) are compatible with the uncertainties in the literature. Also, there is a good agreement between the distribution of the synthetic alpha elements versus ultra-violet excesses and the ones obtained via our calibrations.

Keywords (stars:) late-type - dwarfs - abundances (techniques:) photometric (methods:) statistical (Galaxy:) Globular clusters

S. Karaali

[1]Istanbul University, Faculty of Science, Department of Astronomy and Space Sciences, 34119 University, Istanbul, Turkey

E. Yaz Gökçe

[1]Istanbul University, Faculty of Science, Department of Astronomy and Space Sciences, 34119 University, Istanbul, Turkey

S. Bilir

[1]Istanbul University, Faculty of Science, Department of Astronomy and Space Sciences, 34119 University, Istanbul, Turkey

1 Introduction

Metallicity is one of the means to investigate the formation and evolution of our Galaxy. Metallicity of a star can be determined by spectroscopic measures of its surface, and it is thought to represent the chemical composition of the gas cloud that collapsed to form it. Different metallicity abundances reveal the formation time of that star. Hydrogen (H) and helium (He) were produced after the Big-bang, while metals (elements heavier than H and He) are products of nuclear reactions interior of the stars. The metals are produced from different sources. Alpha (α) elements which are formed by the fusion of alpha particles (^{4}He-nuclei) and iron element (Fe) are produced from Type II supernovae on short timescales, i.e. 20 Myr (Wyse & Gilmore 1988), while iron-peak elements are produced mainly from Type Ia supernovae on much larger timescales, i.e. a few Gyr. The increase of Fe element by time reduces the [α/Fe] value of the interstellar cloud that produces new stars. Hence, one expects a flat distribution for metal poor and old stars and a negative gradient for relatively metal-rich stars. The relation between the alpha element relative to the iron element, [α/Fe], in terms of classical iron element, [Fe/H], is a universal clock for investigation of the formation and evolution of our Galaxy.

The interpretation of Roman (1955) of the weakness of the metallicity lines in the F- and G- type spectra by comparison of the $B-V$ and $U-B$ colours

for each star could be reduced to a procedure for metallicity determination of a star, i.e. the metallicity of a star can be measured by its ultra-violet excess, $\delta(U-B)$, which is defined as the difference between the $U-B$ colours of a star and a standard one with the same $B-V$ colour. It has been a custom to use the $U-B \times B-V$ two-colour diagram of the Hyades cluster as a standard sequence in ultra-violet excess determinations. However, this procedure should be applied with caution due to the guillotin effect which reduces the ultra-violet excess of the red stars with the same metallicity of bluer ones. Sandage (1969) and Carney (1979) normalized the ultra-violet excess by using the procedure of Wildey et al. (1962). Sandage (1969) compared the $U-B$ colours of maximum abundance (which corresponds to $B-V=0.60$) for 112 stars of large proper motion with that of Hyades for the same $B-V$ colour, and defined 16 "guillotin factors" as follows for normalization the ultra-violet excesses: $f=\delta_{0.6}(U-B)/\delta(U-B)$, where $\delta_{0.6}(U-B)$ and $\delta(U-B)$ are the ultra-violet excesses at $B-V=0.6$ and at a given $B-V$ colour which needs to be normalized.

Other studies followed the pioneer ones, i.e. Carney (1979); Karaali et al. (2003, 2011); Karataş & Schuster (2006); Tunçel Güçtekin et al. (2016). Other researchers calibrated the iron abundance in terms of different photometric indices with different procedures: Walraven & Walraven (1960); Strömgren (1966); Cameron (1985); Buser & Fenkart (1990); Trefzger et al. (1995). The alpha elements -Mg, Ti, Ca, Na, O, Si- became important phenomena in recent years. The researchers plotted these elements either individually or their combinations against iron abundances for a set of star sample and separated them into different populations, i.e. thin disc, thick disc, and halo. All the alpha elements appeared in the literature have been determined by their spectroscopic means. However, this procedure requires high resolution which is limited with the near-by dwarfs. We thought to extend the determination of the alpha elements to larger distances by calibrating them photometrically and it is the main scope of this study.

The first time, we estimated synthetic alpha elements, $[\alpha/Fe]_{syn}$, and ultra-violet excesses, δ_{syn} using the Dartmouth Stellar Evolution Database[1] (Dotter et al. 2008) and compared their distribution with the estimated ones by our calibration. We will see that there is an agreement between two sets of data.

Stars for which the alpha elements are available in the literature were separated into different populations in the corresponding studies. While the metallicity calibrations are free of populations. Hence, we will concern only with the alpha elements but not with population types of the sample stars. We organized the paper as follows: The data are given in Section 2 and the procedure is explained in Section 3. Finally, Section 4 is devoted to a summary and discussion.

2 Data

We have two sets of data in our library. The first one consists of the abundances of different elements of Venn et al. (2004, hereafter V04), Bensby et al. (2014, hereafter B14), Reddy et al. (2006, hereafter R06), Nissen & Schuster (2010, hereafter N10), and Stephens & Boesgaard (2002, hereafter S02). The data of V04 is a collection of the data in 15 studies, eight of which are supplied with kinematics while seven of them are without kinematics. The abundances of 10 elements are present for 780 stars in V04. V04 separated the stars into thin disc (TN), thick disc (TK), and halo (H) populations. The catalogue of B14 includes the abundances of 12 elements for 714 stars, including the iron element [Fe/H]. Kinematical data are also available in this catalogue. R06 measured the abundances of 11 elements, including [Fe/H], for 176 stars and they used them to separate the stars into different populations as in V04. Kinematic data are also available in this catalogue. A similar investigation can be seen in N10 who measured the abundances of eight elements including [Fe/H] for 100 stars. However they used a different notation in separation of the stars into different populations, i.e. TD (thick disc stars), "high-α" and "low-α" stars. S02 covers the abundances of eight elements including [Fe/H] for 56 halo stars. There is a large overlapping of the stars in five studies mentioned above. We gave priority to the stars in V04 and B14 and applied a series of constraints to obtain the final set of data available for alpha element calibration, as explained in the following: we reduced the multiplicity of the stars to a single one, we considered only the stars for which the alpha elements [Mg/Fe], [Ca/Fe], [Ti/Fe], and [Na/Fe] are available, and we omitted the giants and the stars without $U-B$ and $B-V$ colour indices. Thus the number of stars (dwarfs) in this set reduced to 619.

The second set of data is the Hypatia catalogue (Hinkel et al. 2014). This catalogue is a collection of many elements published in 69 studies. The least number of elements measured in these studies is two (Ecuvillon et al. 2006; Caffau et al. 2011), while the

[1] http://stellar.dartmouth.edu/models/

biggest one is 33 (Galeev et al. 2004). The number of stars observed in different studies are also different, i.e. Neuforge-Verheecke & Magain (1997) and Porto de Mello et al. (2008) measured only two stars, while Petigura & Marcy (2011) and Valenti & Fischer (2005) measured as much as 914 and 1002 stars, respectively. The total number of stars in Hypatia catalogue is 8821. However, there are many overlapping stars in different studies (including the ones in the first set mentioned in the first paragraph of this section) whose data are included in this catalogue. We applied the same constraints to the data in the second set which reduced the number of stars to only 43.

Then, we decided to separate 39 dwarfs from the first set and combine them with the 43 ones in the second set for the application of the calibration, and use the remaining 589 dwarfs in the first set for the calibration of the alpha elements. We should emphasize that the mentioned 39 stars are not included in the sample used for the calibration. However, these stars were observed with the sample stars simultaneously. While, the 43 stars taken from the Hypatia catalogue were observed at different times. Thus, we should have a chance to compare the results obtained from the two different sets of stars and discuss their accuracy. We evaluated the mean of the anti-logarithm values of [Mg/Fe], [Ca/Fe], [Ti/Fe] and [Na/Fe] common in all stars and took the logarithm of this mean value for each star which will be called as "α element relative to iron", i.e. [α/Fe], in this study. The authors in the cited studies plotted their alpha elements against the iron elements and interpreted this distribution. One can see this picture in all studies related to the alpha elements, whereby thin disc, thick disc and halo populations are defined. Our aim is different. As stated in the Introduction, one does not need the population types of the sample stars in any metallicity calibration. Hence, we used only the alpha elements of our sample stars and fitted them to their ultra-violet excesses obtained from the UBV data. The $U-B$ and $B-V$ data of these stars are provided from SIMBAD[2] and they were de-reddened by the procedure as explained in the following. The $E(B-V)$ colour excesses were evaluated individually for each star making use of the maps of Schlafly & Finkbeiner (2011), and it was reduced to a value corresponding to the distance of the star by means of the equation of Bahcall & Soneira (1980). Then, the $E(U-B)$ colour excesses were evaluated by the following equation (Garcia et al. 1988);

$$E(U-B) = 0.72E(B-V) + 0.05E^2(B-V). \quad (1)$$

[2]http://simbad.u-strasbg.fr/simbad/sim-fbasic

Finally, the de-reddened $(B-V)_0$ and $(U-B)_0$ colours could be determined by the following equations:

$$(U-B)_0 = (U-B) - E(U-B), \quad (2)$$
$$(B-V)_0 = (B-V) - E(B-V).$$

The stars cover the $(B-V)_0$ colour range $0.325 < (B-V)_0 \leq 0.775$ mag which corresponds to the spectral type range F0-K2. The spectroscopic and photometric data of the stars, as well as their ID numbers, coordinates, and sources are given in Table 1. A detailed inspection of these stars revealed that some of them have some peculiarities, i.e. they are binary, variable, double or multiple, and chromospheric active stars. We did not exclude such stars from the program, however we followed a procedure, explained in Section 3, to omit those with large scatter in the diagram that we used for calibration of the [α/Fe] in terms of ultra-violet excess.

3 The Procedure

The procedure consists of calibration of the [α/Fe] element in terms of ultra-violet excess $\delta(U-B)_0$, the difference between $(U-B)_0$ colours of a given star and the Hyades star with the same $(B-V)_0$ colour. $\delta(U-B)_0$ excess is related to a bulk heavy metal abundance which is denoted as [M/H] in the literature, and [M/H] can be related to other indicators for various components of the Milky Way Galaxy. These indicators cover small group of elements, where [Fe/H] is the most favorite indicator in question. Thus, as stated in the Introduction, [Fe/H] could be calibrated in terms of $\delta(U-B)_0$ and the iron abundances of the dwarf stars in our Galaxy could be determined. Here, the indicator will be the [α/Fe] element which covers the elements [Mg/Fe], [Ca/Fe], [Ti/Fe], [Na/Fe]. Stars with different $(B-V)_0$ colours with the same metal abundance show different values of ultra-violet excess due to the shapes of the blanketing vectors as stated in the Introduction. For late-type stars, $\delta(U-B)_0$ is partially guillotined because the blanketing line is nearly parallel to the intrinsic Hyades line. Hence, the ultra-violet excesses of stars used in the calibration of any metallicity should be normalized. This is the case in Sandage (1970) and Karaali et al. (2003, 2005, 2011) where all ultra-violet excesses were reduced to the ultra-violet excess at $(B-V)_0 = 0.6$ mag, $\delta_{0.6}(U-B)_0$. There is a slight different procedure for calibration of [α/Fe] and any metallicity in terms of (*unreduced*) ultra-violet excess, i.e. one can fit the [α/Fe] values to the $\delta(U-B)_0$ ultra-violet excesses for a sample of stars with limited $(B-V)_0$ colour-range. This is the procedure we used in this study. We separated the colour interval $0.325 < (B-V)_0 \leq 0.775$ mag

into nine sub-intervals, i.e. $0.325 < (B-V)_0 \leq 0.375$, $0.375 < (B-V)_0 \leq 0.425$, ..., and $0.725 < (B-V)_0 \leq 0.775$ mag. Thus we obtained nine sub-samples of stars for calibration of [α/Fe] in terms of $\delta(U-B)_0$ (hereafter we will use the notation δ). The scales of the sub-intervals are equal, $\Delta(B-V)_0 = 0.05$ mag, and they are larger than the errors in the $(U-B)_0$ and $(B-V)_0$ colours.

3.1 Calibration of [α/Fe] in terms δ

We separated the stars in Table 1 into nine sub-samples as stated in the preceding paragraph and calibrated the [α/Fe] elements in terms of ultra-violet excesses δ for stars in each sub-sample as explained in the following. Each calibration is carried out in three steps. In the first step, we rejected the stars which show large scatter in the [α/Fe] - δ diagram. These stars are candidates for binarity, variable, double or multiple, and chromospheric active stars. Then, we fitted the [α/Fe] element in terms of δ (first calibration) for the remaining sample stars and reproduced the alpha elements of the stars in this reduced sample by replacing their ultra-violet excesses into the first calibration. We use the symbol $[\alpha/Fe]_{rep}$ for the alpha elements reproduced by the first calibration. Then, we estimated the residuals, the differences between the (original) [α/Fe] elements and [α/Fe]$_{rep}$, and the corresponding standard deviation, σ.

In the second step we omitted stars with (original) [α/Fe] elements which lie out of the interval [α/Fe]$_{rep} \pm \Delta$[α/Fe], where Δ[α/Fe] corresponds to the mean of the residuals larger than the standard deviation, σ. Thus, we re-reduced the original star sample for the second time and (in the third step) we calibrated the (original) [α/Fe] element in terms of δ. This is our second and final calibration for a sub-sample. The results are given in Fig. 1. The stars rejected in the first step and omitted in the second step are shown by an asterisk and a triangle, respectively, while filled circles indicate the stars used in the final calibration.

The total number of stars used in our (final) calibrations is 469. We adopted a third degree polynomial in our calibrations as in the following:

$$[\alpha/Fe] = a_3\delta^3 + a_2\delta^2 + a_1\delta^1 + a_0. \quad (3)$$

The numerical values of the coefficients a_i ($i = 0, 1, 2, 3$) for all the stars except the rejected ones are given in Table 2, while those for the re-reduced sub-sample (the final one without rejected and omitted stars) are presented in Table 3. The coefficients which will be used for the estimation of the alpha elements via the ultra-violet excess are the ones in Table 3.

3.2 Application of the Procedure

We applied the procedure to two sets of field stars and two sets of clusters. The first set of field stars consists of 43 stars taken from the Hypatia catalogue (Hinkel et al. 2014), while the second one is a combination of stars in Bai et al. (2004, hereafter Bai04):10, B14: 12, V04: 7, S02: 5, N10: 3, and R06: 2, totally 39 stars. The difference between these sets of stars is that 29 stars in B14, V04, S07, N10 and R06 are taken from the same source of stars used for the calibration of the [α/Fe] element. However, they are not included into the sample used for the calibration, as stated in Section 2. We evaluated the ultra-violet excesses (δ) of the stars in both sets by using their UBV data provided from SIMBAD and the procedure in Section 2, and replaced them into our final calibration to calculate an alpha element, [α/Fe]$_{cal}$, for each star. Now, we need the original alpha elements, [α/Fe]$_{org}$, of the stars in question which are based on spectroscopic means to test the accuracy of the calculated alpha elements. We evaluated the mean of the anti-logarithmic values of the [Mg/Fe], [Ca/Fe], [Ti/Fe] and [Na/Fe] elements common in the stars for each set and took the logarithm of the mean value for each star for our purpose.

The results for the first set of the field stars taken from the Hypatia catalogue are given in Table 4a. The mean of the residuals, Δ[Fe/H]=[α/Fe]$_{org}$-[α/Fe]$_{cal}$, and the corresponding standard deviation are $\langle\Delta[\alpha/Fe]\rangle$=-0.090 and $\sigma = 0.102$ dex, respectively. The results for the second set of the field stars, taken from the same source of the stars used for the calibration of the [α/Fe], are tabulated in Table 4b. The mean of the residuals and the corresponding standard deviation are $\langle\Delta[\alpha/Fe]\rangle$=-0.009 and $\sigma = 0.079$ dex, respectively. One can see that the mean of the residuals is rather small, and the standard deviation is smaller than the one 43 field star.

Dias et al. (2016) measured the iron abundance [Fe/H] and alpha element [α/Fe] for 51 globular clusters in their FORS2/VLT survey. We used this advantage to apply our calibrations to two sets of globular clusters as explained in the following. We could provided the $B-V$ and $U-B$ colour indices for 25 of these clusters from the catalogue of Harris (2010), and for 19 clusters from Hanes & Brodie (1985). The restriction of the number of clusters is due to the constraint of the range of the $(B-V)_0$ colour index of our calibration, i.e. $0.325 < (B-V)_0 \leq 0.775$ mag. The $B-V$ and $U-B$ colour indices for 16 clusters are available in both sets. However, the values of a given colour index for a cluster are different in two sets which cause different residuals as it is shown in the following.

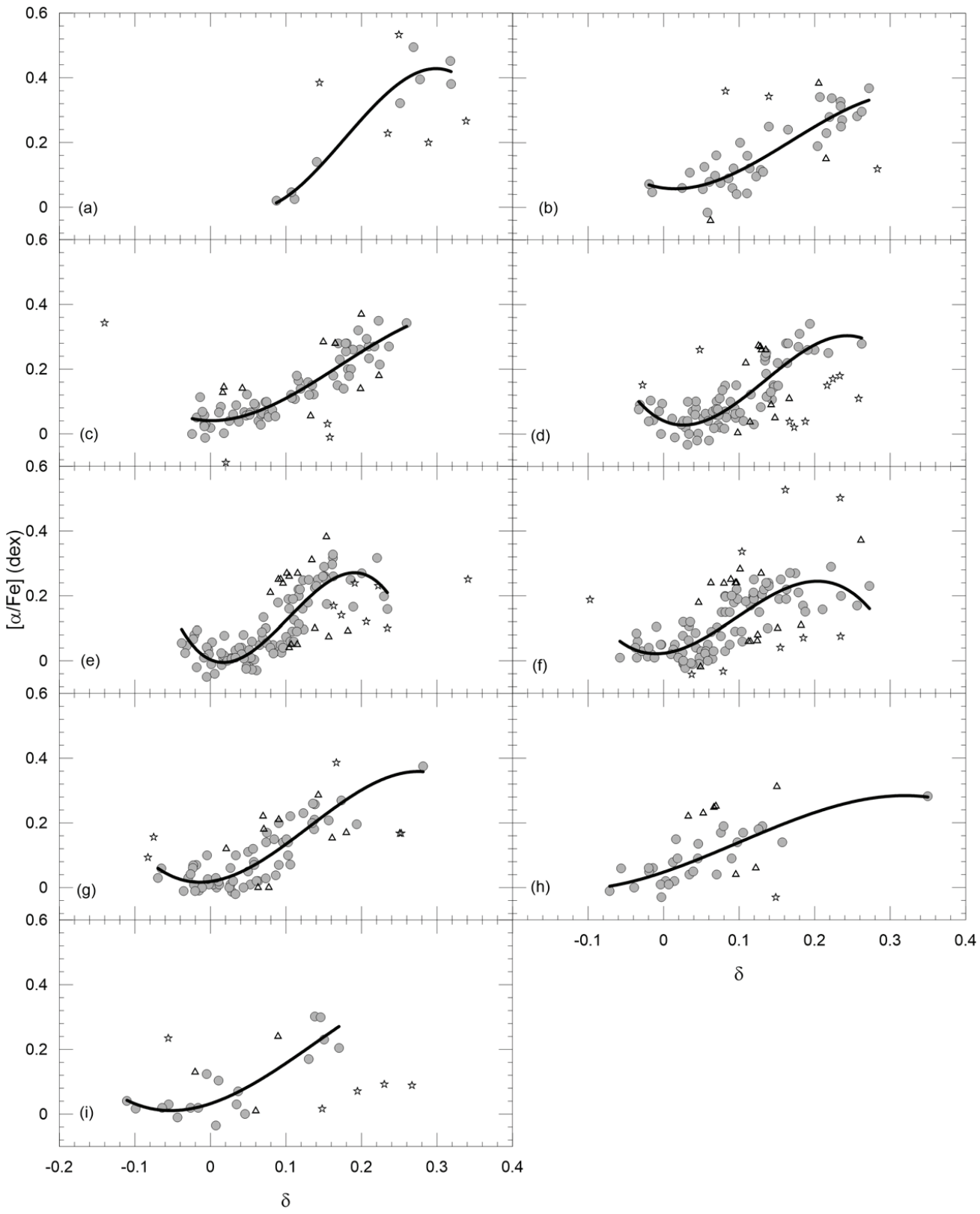

Fig. 1 Calibration of the [α/Fe] element in terms of δ for nine sub-samples: (a) $0.325 < (B-V)_0 \leq 0.375$, (b) $0.375 < (B-V)_0 \leq 0.425$, (c) $0.425 < (B-V)_0 \leq 0.475$, (d) $0.475 < (B-V)_0 \leq 0.525$, (e) $0.525 < (B-V)_0 \leq 0.575$, (f) $0.575 < (B-V)_0 \leq 0.625$, (g) $0.625 < (B-V)_0 \leq 0.675$, (h) $0.675 < (B-V)_0 \leq 0.725$, (i) $0.725 < (B-V)_0 \leq 0.775$ mag. An asterisk indicates the star with large scattering which is rejected from the program (first step in the text), a triangle indicates the star which lies out of the interval $[\alpha/\mathrm{Fe}]_{rep} \pm \Delta$ [α/Fe] and which is omitted in the final calibration (second step in the text), and a filled circle indicates the star considered in the final calibration (third step in the text). The symbols $[\alpha/Fe]_{rep}$ and Δ [α/Fe] are explained in the text.

The data for the 25 clusters of the first set whose $B-V$ and $U-B$ colour indices are taken from Harris (2010) are given in Table 4c. The de-reddened colours are evaluated by using the colour excess $E(B-V)$ in Harris (2010), the ultra-violet index for the Hyades cluster, $(U-B)_H$, the ultra-violet excess, δ, and the $[\alpha/\mathrm{Fe}]_{cal}$ are estimated by the same procedures used in the preceding paragraphs. The mean of the residuals, Δ[Fe/H]=$[\alpha/\mathrm{Fe}]_{org}$-$[\alpha/\mathrm{Fe}]_{cal}$, and the corresponding standard deviation are $\langle\Delta[\alpha/\mathrm{Fe}]\rangle$=0.073 and σ = 0.091 dex.

The data for 19 clusters for the second set are presented in Table 4d. The errors for $B-V$ of three clusters and for $U-B$ of 11 clusters are also given in Hanes & Brodie (1985). We considered the errors tabulated in Table 4d for six clusters to obtain smaller residuals in [α/Fe] for them, while for five clusters the residuals are already small and one does not need any correction in $B-V$ or $U-B$ colour indices. The mean of the residuals and the corresponding standard deviation for the second set of the clusters are much better than for the first set, i.e. $\langle\Delta[\alpha/\mathrm{Fe}]\rangle$=-0.012 and σ = 0.053 dex, respectively.

3.3 Synthetic Alpha Elements and UV-Excesses

We estimated synthetic alpha elements, $[\alpha/\mathrm{Fe}]_{syn}$, and ultra-violet excesses, δ_{syn}, for nine sub-samples, i.e. $0.325 < (B-V)_0 \leq 0.375$, $0.375 < (B-V)_0 \leq 0.425$, ..., $0.725 < (B-V)_0 \leq 0.775$ mag, using the Dartmouth Stellar Evolution Program (DSEP, Dotter et al. 2008) and compared their distribution with the ones estimated by our calibration, as explained in the following. We took the DSEP isochrones and did the necessary interpolations to get the required data for the relations. The estimations of $[\alpha/\mathrm{Fe}]_{syn}$ and δ_{syn} are carried out for three populations, thin disc, thick disc and halo whose metallicity ranges are assumed to be -0.5<[Fe/H]≤ +0.5, -1.0≤ [Fe/H]<-0.5 and -2.5≤ [Fe/H]<-1.0 dex, respectively. Also, we adopted the 3, 12 and 13 Gyr as the ages of the populations in the same order. Thus, we estimated a set of $(B-V, U-B)$ couples for each population using an iron abundance, an $[\alpha/\mathrm{Fe}]_{syn}$ value and an age value, each time. The range of the $[\alpha/\mathrm{Fe}]_{syn}$ is adopted as -0.2≤$[\alpha/\mathrm{Fe}]_{syn}$ ≤ +0.8. The iron metallicity and $[\alpha/\mathrm{Fe}]_{syn}$ are used in 0.5 and 0.2 dex steps, respectively. Finally, we considered only the $B-V$ and $U-B$ colour indices which lie in the $(B-V)_0$ range of our sample, i.e. $0.325 < (B-V)_0 \leq 0.775$ dex. The ultra-violet excesses are estimated relative to the ultra-violet index for [Fe/H]=0.0 dex. The distributions of the $[\alpha/\mathrm{Fe}]_{syn}$ and δ_{syn}, are plotted in Fig. 2. The mean $(B-V)_0$ colour index and a colour coded symbol are also indicated for each sub-sample. We could fit the data in Fig. 2 to a third degree polynomial with a high correlation coefficient ($R^2 = 0.987$): $[\alpha/\mathrm{Fe}]_{syn} = -22.827 \times \delta_{syn}^3 + 10.604 \times \delta_{syn}^2 + 0.264 \times \delta_{syn} + 0.017$. Finally, we plotted our calibrations obtained for nine sub-samples and the one for synthetic data in the same diagram for comparison purpose. Fig. 3 shows that the calibration curves and the synthetic one have the same trend. Also, for $\delta_{syn} < 0.18$ the synthetic curve lies within the region occupied by the calibration curves. Although the synthetic curve for larger δ_{syn} occupies the alpha elements which are a bit larger than the ones corresponding to the calibration curves, an additional error of $\Delta[\alpha/\mathrm{Fe}]$=0.10 dex to our calibrations supplies an agreement also for this segment. The agreement of the synthetic calibration with the ones based on the measured alpha elements indicates that the alpha abundances of individual stars can be determined via their UV excesses.

4 Summary and Discussion

We present the calibration of the [α/Fe] element in terms of the ultra-violet excess, δ, for dwarf stars in nine sub-samples, defined by the $(B-V)_0$ colours with a range of $\Delta(B-V)_0 = 0.050$, i.e. $(0.325, 0.375]$, $(0.375, 0.425]$, ..., and $(0.725, 0.775]$. We fitted a third degree polynomial for our calibration, a procedure that we used in Karaali et al. (2003, 2005, 2011) for calibration of the iron abundance, [Fe/H]. The difference between our study and the cited ones is that in the previous studies all the ultra-violet excesses were normalized to the colour $(B-V)_0 = 0.6$, and only a single calibration equation was derived for all the data. Whereas, here we preferred to use the ultra-violet excess estimated for the colour of the star. However, we separated the stars into sub-samples with limited $(B-V)_0$ range to avoid any guillotin effect mentioned in Section 3. The lower limit of the [α/Fe] element in our calibrations is ~ 0 for all $(B-V)_0$ intervals, while the upper limits for the blue colours $(0.325, 0.375]$, $(0.375, 0.425]$, and $[0.425, 0.475]$ are larger than the ones for redder colours. Our calibrations provide [α/Fe] elements in the range (0.0, 0.4], which cover the elements of the thin disc, thick disc and some halo stars.

We applied the procedure to two sets of field stars and two sets of clusters. The mean of the residuals and the corresponding standard deviation for 43 field stars taken from Hypatia catalogue (Hinkel et al. 2014) are $\langle\Delta[\alpha/\mathrm{Fe}]\rangle$=-0.090 and σ = 0.102 dex, while those for the second set of 39 field stars which are taken from

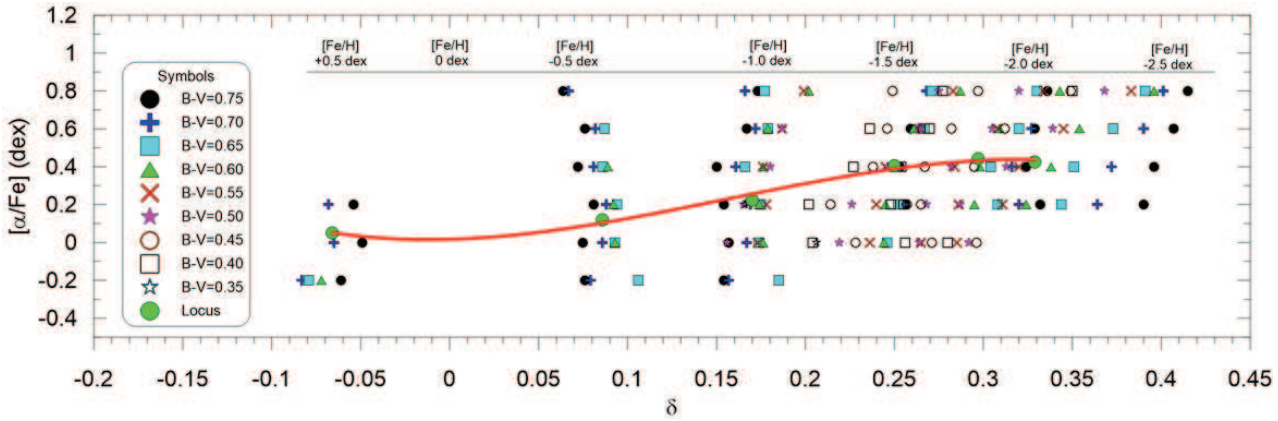

Fig. 2 ($[\alpha/Fe]_{syn}$, δ_{syn}) diagram for a set of iron metallicity which covers thin disc, thick disc, and halo populations.The curve indicates the third degree polynomial fitted to the data. The range of the synthetic alpha element is -0.2≤$[\alpha/Fe]_{syn}$ ≤ +0.8 dex. The colour coded symbols are explained in the text.

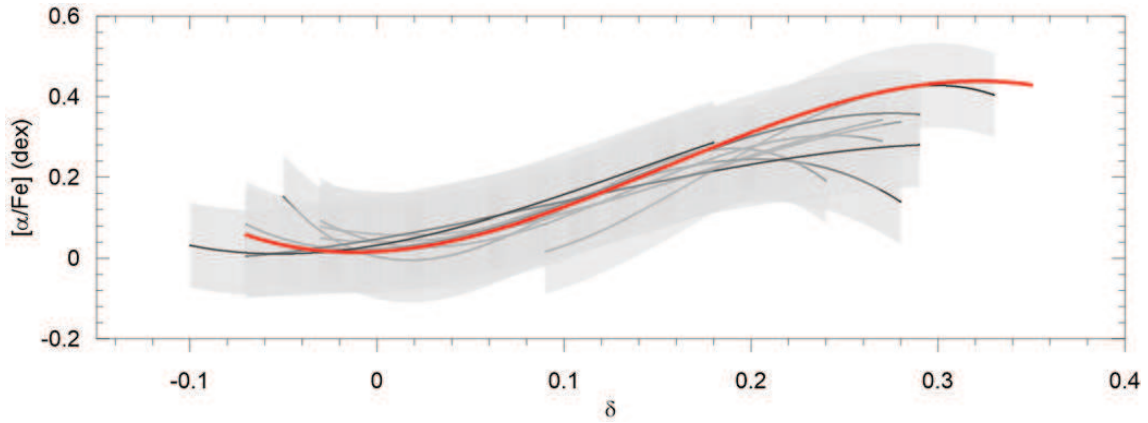

Fig. 3 Comparison of the calibration based on the synthetic alpha elements and ultra-violet excesses, $[\alpha/Fe]_{syn}$ and δ_{syn} (red curve), with the calibrations obtained for nine sub-samples. The shadowed area corresponds to nine calibrations with 0.10 uncertainty in $[\alpha/Fe]_{syn}$.

Bai04, B14, V04, S02, N10 and R06 are $\langle\Delta[\alpha/Fe]\rangle$=-0.009 and $\sigma = 0.079$ dex. We compared the numerical values of alpha elements estimated for a star by different researchers to test the accuracy of our results. The data for [Mg/Fe], [Ca/Fe], and [Ti/Fe] elements in Table 5a are taken from Bai04, while their mean, [α/Fe], is estimated in this study. One can see that the differences between the numerical values for the cited elements determined by Bai04, F00, and S02 can be as large as 0.20 and 0.30 dex. There are also differences between the numerical values of [α/Fe] elements determined by V04, B14, N10, and R06, however not larger than $\sim$ 0.10 dex (Table 5b). It seems that the accuracy of the $[\alpha/Fe]_{cal}$ elements for the 43 Hypatia stars is compatible to the one for the alpha elements in Table 5a,while the $[\alpha/Fe]_{cal}$ elements estimated for the 39 stars in the second set are more accurate and their accuracy is compatible to the alpha elements in Table 5b. 39 stars with more accurate $[\alpha/Fe]_{cal}$ elements were measured with the sample stars simultaneously which indicates (a small) bias, i.e. the accuracy of the alpha elements depends also on the procedure used in their observations.

We applied the procedure also to two sets of globular clusters whose [α/Fe] elements are taken from the same study (Dias et al. 2016). Harris (2010) catalogue provides $B-V$ and $U-B$ colour indices for 25 clusters for the application of our calibration, while the number of clusters in Hanes & Brodie (1985) with different $B-V$ and $U-B$ colours available for our purpose is 19. The colour excesses, $E(B-V)$, for all clusters are taken from Harris (2010). We expect from this procedure to find out the reason of any probable difference in accuracy for the estimated alpha elements in two sets. The mean of the residuals and the corresponding standard deviation for 25 clusters in the first set are $\langle\Delta[\alpha/Fe]\rangle$=0.073 and $\sigma = 0.091$ dex, while the ones for 19 clusters in the second set are $\langle\Delta[\alpha/Fe]\rangle$=-0.012 and $\sigma = 0.053$ dex, respectively. One can see that there are considerable differences between the mean of the residuals, and standard deviations for two set of clusters. We used the same calibrations to estimate the $[\alpha/Fe]_{cal}$. Hence the differences in question should originate from the data used in two sets. Original alpha elements, [α/Fe], are taken from the same study. Additionally there are 16 clusters common in two sets which means that 16 residuals in two sets are estimated by the same [α/Fe] elements. All the colour excesses, $E(B-V)$, are taken from the same source, and the ultra-violet index for the Hyades cluster, $(U-B)_H$, is estimated by the same equation. Then, it remains the $B-V$ and $U-B$ colour indices which cause different residuals and standard deviations. The residuals, Δ[α/Fe], for 16 clusters in the first set (Table 4c) are added to the last column of Table 4d for comparison purpose. One can see that different $B-V$ and $U-B$ colour indices of a star may cause a difference in the residual as much as 0.18 dex. One can generalize this result obtained via the clusters, i.e. the accuracy of an estimated alpha element for a star depends on the accuracy of the $B-V$ and $U-B$ colour indices of that star.

As stated in Section 2, most of the stars used for the calibration of the procedure are taken from B14 (238 stars) and V04 (283 stars). The errors for the elements [Mg/Fe], [Ca/Fe], [Ti/Fe] and [Na/Fe] were not given in V04, while they are present in B14. We used them and estimated the propagated error for the alpha element, [α/Fe], for all stars (714 stars) in B14 and showed their distribution in Fig. 4. The mean and the standard deviation for the errors in question are $\langle$ $[\alpha/Fe]_{err}\rangle$= 0.147 and $\sigma = 0.094$ dex, respectively. However, the propagated errors for the majority of the stars are less than 0.15 dex.

We thought that it would be useful to plot the differences between the original and estimated alpha elements in a figure. This is carried out in Fig. 5, where panels (a), (b), (c) and (d) cover the distributions of

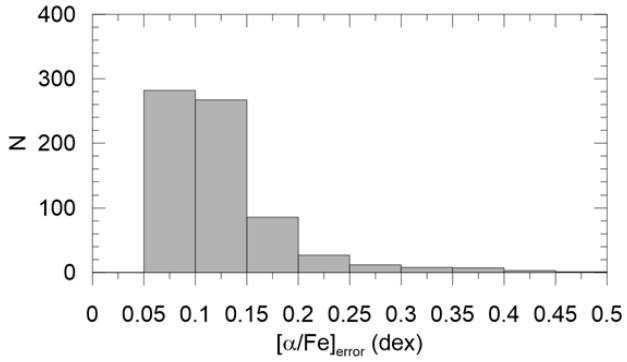

Fig. 4 Distribution of the propagated errors for the [α/Fe] element for the stars in B14.

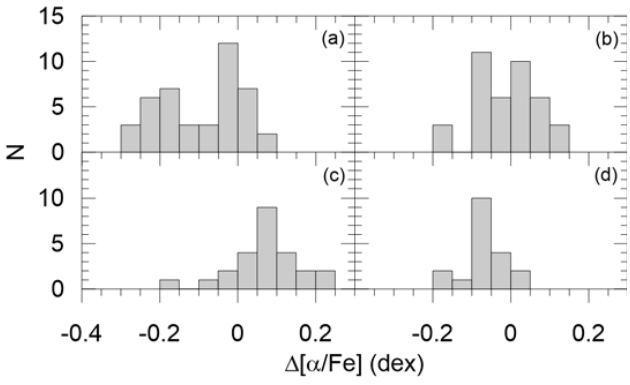

Fig. 5 Histograms of the residuals, Δ[α/Fe], in Tables 4a, 4b, 4c and 4d.

the residuals, Δ[Fe/H]=[α/Fe]$_{org}$-[α/Fe]$_{cal}$, in Tables 4a, 4b, 4c, and 4d, respectively. One can see that the absolute values of the residuals for the majority of the stars in four panels are less than 0.15 dex, a numerical value equals to the maximum propagated error for the original alpha elements for most of the stars in B14. Statistics of the residuals (absolutely) less than 0.15 as well as 0.20 dex are given in Table 6. We estimated synthetic alpha elements and UV - excesses too. There is an agreement between the synthetic calibration and the observed ones within Δ[α/Fe]=0.10 dex accuracy.

Conclusion: The accuracy of the alpha elements estimated in our calibration and the agreement of the synthetic calibration with our calibration based on the measured alpha elements confirm our argument that alpha abundances of individual stars based on the UV excess of stars can be constrained.

Acknowledgments

Authors are grateful to the anonymous referee for his/her considerable contributions to improve the paper. This research has made use of NASA (National Aeronautics and Space Administration)'s Astrophysics Data System and the SIMBAD Astronomical Database, operated at CDS, Strasbourg, France.

References

An, D., et al., 2008, ApJS, 179, 326
Bai, G. S., Zhao, G., Chen, Y. Q., et al., 2004, A&A, 425, 671
Bahcall, J. N., Soneira, R. M., 1980, ApJS 44, 73
Bensby, T., Feltzing, S., Oey, M. S., 2014, A&A, 562, A71
Buser, R., Fenkart, R. P., 1990, A&A, 239, 243
Caffau, E., Bonifacio, P., Francois, P., et al., 2011, Natur, 477, 67
Cameron, L. M., 1985, A&A, 152, 250
Cannon, R. D., 1974, MNRAS, 167, 551
Carney, B. W., 1979, AJ, 84, 515
Cheng, J. Y., Rockosi, C. M., Morrison, H. L., et al., 2012, ApJ, 752, 51
Chiappini, C., 2001, AmSci, 89, 506
Dias, W. S., Alessi, B. S., Moitinho, A., Lépine, J. R. D., 2002, A&A, 389, 871
Dias, B., Barbuy, B., Saviane, I., Held, E. V., Da Costa, G. S., Ortolani, S., Gullieuszik, M., Vasquez, S., 2016, A&A, 590, 9
Di Cecco, A., Bono, G., Prada Moroni, P. G., et al., 2015, AJ, 150, 51
Dotter, A., Chaboyer, B., Jevremovic, D., Kostov, V., Baron, E., Ferguson, J. W., 2008, ApJS, 178, 89
Ecuvillon, A., Israelian, G., Santos, N. C., Mayor, M., Gilli, G., 2006, A&A, 449, 809E
Eggen, O. J., Iben, I. Jr., 1989, AJ, 97, 431
Fulbright, J. P., 2000, AJ, 120, 1841
Garcia, B., Claria, J.J., Levato, H., 1988, ApSS, 143, 317
Galeev, A. I., Bikmaev, I. F., Musaev, F. A., Galazutdinov, G. A., 2004, ARep, 48, 492
Gilmore, G., Randich, S., Asplund, M., et al., 2012, The Messenger, 147, 25
Gratton, R. G., Fusi Pecci, F., Carretta, E., et al., 1997, ApJ, 491, 749
Hanes, D. A., Brodie, J. P., 1985, MNRAS, 214, 491
Harris, W. E., 2010, arXiv:1012.3224
Hiltner, W. A., Johnson, H. L., 1956, ApJ, 124, 367
Hinkel, N. R., Timmes, F. X., Young, P. A., Pagano, M. D., Turnbull, M. C., 2014, AJ, 148, 54
Hodder, P. J. C., Nemec, J. M., Richer, H. B., Fahlman, G. G., 1992, AJ, 103, 460
Ishigaki, M. N., Aoki, W., Chiba, M., 2013, ApJ, 771, 67
Jacobson, H. R., Pilachowski, C. A., Friel, E. D., 2011, AJ, 142, 59
Karaali, S., Bilir, S., Karataş, Y., Ak, S. G., 2003, PASA, 20, 165
Karaali, S., Bilir, S., Tunçel, S., 2005, PASA, 22, 24
Karaali, S., Bilir, S., Ak, S., Yaz, E., Coşkunoğlu, B., 2011, PASA, 28, 95
Karataş, Y., Schuster, W., 2006, MNRAS, 371, 1793
Latham, D. W., Stefanik, R. P., Torres, G., et al., 2002, AJ, 124, 1144
Lee, Y. S., Beers, T. C., Allende Prieto, C., et al., 2011b, AJ, 141, 90
Lu, P. K., Demarque, P., van Altena, W., McAlister, H., Hartkopf, W., 1987, AJ, 94, 1318
Neuforge-Verheecke, C., Magain, P., 1997, A&A, 328, 261
Nissen, P. E., Schuster, W. J., 2010, A&A, 511L, 10
Nissen, P. E., Schuster, W. J., 2011, A&A, 530, A15
Pace, G., 2013, A&A, 551L, 8
Petigura, E. A., Marcy, G. W., 2011, ApJ, 735, 41
Porto de Mello, G. F., Lyra, W., Keller, G. R., 2008, A&A, 488, 653
Ramírez, I., Allende Prieto, C., Lambert, D. L., 2013, ApJ, 764, 78
Reddy, B. E., Lambert, D. L., Allende Prieto, C., 2006, MNRAS, 367, 1329
Richer, H. B., Harris, W. E., Fahlman, G. G., et al., 1996, ApJ, 463, 602
Roman, N. G., 1955, ApJS, 2, 195
Rose, J. A., 1984, AJ, 89, 1238
Sandage, A., 1969, ApJ, 158, 1115
Sandage, A., 1970, ApJ, 162, 841
Sanders, W. L., 1989, RMxAA, 17, 31
Santos, J. F. C., Jr. Piatti, A. E., 2004, A&A, 428, 79
Schlafly, E. F., Finkbeiner, D. P., 2011, ApJ, 737, 103
Stephens, A., Boesgaard, A. M., 2002, AJ, 123, 1647
Stetson, P. B., McClure, R. D., VandenBerg, D. A., 2004, PASP, 116, 1012
Strömgren, B., 1966, ARA&A, 4, 433
Torres, S., García-Berro, E., Althaus, L. G., Camisassa, M. E., 2015, A&A, 581, A90
Trefzger, Ch. F., Pel, J. W., Gabi, S., 1995, A&A, 304, 381
Tunçel Güçtekin S., Bilir S., Karaali S., Ak S., Ak T., Bostancı Z. F., 2016, Ap&SS, 361, 186
Wyse, R. F. G., Gilmore, G., 1988, AJ, 95, 1404
Valenti, J. A., Fischer, D. A., 2005, ApJS, 159, 141
Venn, K. A., Irwin, M., Shetrone, M. D., et al., 2004, AJ, 128, 1177
Walraven, Th., Walraven, J. H., 1960, Bulletin of the Astronomical Institutes of the Netherlands, 15, 67
Wildey, R. L., Burbidge, E. M., Sandage, A. R., Burbidge, G. R., 1962, ApJ, 135, 94

This manuscript was prepared with the AAS LaTeX macros v5.2.

Table 1 Data for 589 program stars. The columns give: current number (N), ID, equatorial coordinates (α, δ), Galactic coordinates (l, b), parallax (π) and its error (π_{err}), colour excess ($E(B-V)$), $B-V$ and $U-B$ colours, de-reddened $(B-V)_0$ and $(U-B)_0$, effective temperature (T_e), surface gravity ($\log g$), iron abundance ([Fe/H]), alpha element ([α/Fe]), remarks, ultra-violet colour corresponding Hyades squence, $(U-B)_H$, for a given $(B-V)_0$ colour, ultra-violet excess (δ), and Remark

N	ID	α (hh:mm:ss.ss)	δ (dd:mm:ss.s)	l (^{o})	b (^{o})	π (mas)	π_{err} (mas)	$E(B-V)_r$ (mag)	$B-V$ (mag)	$U-B$ (mag)	$(U-B)_0$ (mag)	$(B-V)_0$ (mag)	T_e (K)	$\log g$ (cgs)	[Fe/H] (dex)	[α/Fe] (dex)	Ref. (dex)	Rem.	Ref	$(U-B)_H$ (mag)	δ (mag)	Remark
1	HIP 36513	07:30:41.30	+24:05:10.0	194.9332	18.939	2.57	2.32	0.031	0.357	-0.220	-0.242	0.326	–	–	-2.55	0.38	V04	HP	–	0.077	0.32	considered
2	HIP 96115	19:32:31.90	+26:23:26.0	60.9206	3.4682	7.25	1.35	0.054	0.389	-0.218	-0.257	0.335	–	–	-2.41	0.45	V04	HP	–	0.061	0.32	considered
3	HIP 47048	09:35:16.70	−49:07:48.9	273.2968	2.117	10.26	0.95	0.032	0.398	-0.095	-0.118	0.366	6630	4.12	-0.50	0.14	B14	–	–	0.023	0.14	considered
.	.	.	.	.	.	.	.	.	.	.	.	.	.	.	.	.	.	.	.	.	.	.
.	.	.	.	.	.	.	.	.	.	.	.	.	.	.	.	.	.	.	.	.	.	.
.	.	.	.	.	.	.	.	.	.	.	.	.	.	.	.	.	.	.	.	.	.	.
588	HIP 68101	13:56:32.90	−54:42:17.0	312.3222	6.9756	25.84	0.48	0.012	0.780	0.230	0.222	0.768	–	–	-0.53	0.02	V04	HP	–	0.37	0.15	scattered
589	HIP 50713	10:21:16.79	−17:02:55.4	259.0917	32.7519	16.48	1.14	0.014	0.786	0.327	0.317	0.772	5263	4.46	-0.11	0.01	B14	CA	Pace+2013	0.38	0.06	omitted

Table 2 Numerical values for the coefficients a_i $(i = 0, 1, 2, 3)$ used for the calibration of $[\alpha/Fe]$ element in the first step. N indicates the number of stars in each $(B-V)_0$ colour range, σ is the standard deviation and R^2 is the squared correlation coefficient.

$(B-V)_0$	a_3	a_2	a_1	a_0	R^2	σ	N
$(0.325, 0.375]$	-60.955	32.423	-3.0600	0.0739	0.9483	0.044	9
$(0.375, 0.425]$	-27.357	12.810	-0.4762	0.0550	0.7470	0.057	39
$(0.425, 0.475]$	-17.539	8.6445	-0.0163	0.0484	0.7569	0.048	75
$(0.475, 0.525]$	-52.911	21.120	-0.9557	0.0406	0.6345	0.056	86
$(0.525, 0.575]$	-99.929	29.822	-0.7230	0.0062	0.6290	0.065	106
$(0.575, 0.625]$	-26.470	7.5664	0.5794	0.0331	0.5142	0.065	102
$(0.625, 0.675]$	-23.075	8.9882	0.4327	0.0251	0.6697	0.056	68
$(0.675, 0.725]$	-0.7373	-0.9143	1.0304	0.0636	0.4572	0.067	35
$(0.725, 0.775]$	-9.9681	5.5567	0.7237	0.0411	0.6725	0.060	21

Table 3 Numerical values for the coefficients a_i $(i = 0, 1, 2, 3)$ used in the final calibration of [α/Fe] element. N indicates the number of stars in each $(B-V)_0$ colour range, σ is the standard deviation and R^2 is the squared correlation coefficient. The domain of the [α/Fe] is also given in the second column. Errors of coefficients are given in parentheses.

$(B-V)_0$	δ	a_3	a_2	a_1	a_0	R^2	σ	N
(0.325, 0.375]	[0.087, 0.319]	-60.9550(60.7871)	32.4230(39.1548)	-3.0600(7.8686)	0.0739(0.4694)	0.9483	0.044	9
(0.375, 0.425]	[-0.019, 0.272]	-20.3210(17.1027)	10.2980(6.3506)	-0.2996(0.6472)	0.0600(0.0233)	0.7980	0.048	36
(0.425, 0.475]	[-0.024, 0.260]	-17.3710(10.7474)	8.9305(3.5685)	-0.0272(0.3162)	0.0407(0.0085)	0.8601	0.036	66
(0.475, 0.525]	[-0.033, 0.262]	-54.1660(11.9521)	21.8760(3.8644)	-1.0355(0.3400)	0.0410(0.0104)	0.7478	0.045	76
(0.525, 0.575]	[-0.038, 0.234]	-105.8600(13.6112)	33.0280(4.0198)	-1.0470(0.3032)	0.0038(0.0087)	0.7883	0.047	91
(0.575, 0.625]	[-0.058, 0.273]	-45.7050(9.3323)	13.2730(2.9961)	0.2801(0.2394)	0.0233(0.0089)	0.6809	0.050	86
(0.625, 0.675]	[-0.070, 0.282]	-28.3440(8.2069)	11.1100(2.6058)	0.3240(0.1900)	0.0190(0.0083)	0.7659	0.044	59
(0.675, 0.725]	[-0.071, 0.350]	-6.8017(7.8702)	2.0239(3.1811)	0.7881(0.2338)	0.0477(0.0113)	0.6888	0.042	28
(0.725, 0.775]	[-0.110, 0.170]	-14.9820(32.1468)	6.2218(3.0120)	0.7757(0.4553)	0.0324(0.0189)	0.7721	0.051	18

Table 4a Data for 43 field stars taken from the Hypatia catalogue and used for the application of the procedure. The columns give: Hipparcos number, galactic coordinates (l, b), parallax (π), reduced colour excess ($E_d(B-V)$), iron metallicity ([Fe/H]), de-reddened colours ($(B-V)_0$ and $(U-B)_0$), ultra-violet index for the Hyades cluster ($(U-B)_H$), ultra-violet excess (δ), original alpha element ($[\alpha/\mathrm{Fe}]_{org}$), calculated alpha element ($[\alpha/\mathrm{Fe}]_{cal}$), and the residual ($\Delta[\alpha/\mathrm{Fe}]$).

HIP	l	b	π	$E_d(B-V)$	[Fe/H]	$(B-V)_0$	$(U-B)_0$	$(U-B)_H$	δ	$[\alpha/\mathrm{Fe}]_{org}$	$[\alpha/\mathrm{Fe}]_{cal}$	$\Delta[\alpha/\mathrm{Fe}]$
	(^{o})	(^{o})	(mas)	(mag)	(dex)	(mag)	(mag)	(mag)	(mag)	(dex)	(dex)	(dex)
1382	323.11	-71.91	27.51±0.64	0.001	-0.06	0.652	0.089	0.190	0.101	-0.14	0.14	-0.28
6744	231.77	-81.87	23.27±0.92	0.004	0.12	0.731	0.237	0.306	0.069	-0.11	0.11	-0.22
6762	141.97	-61.71	34.07±1.00	0.004	–	0.734	0.302	0.311	0.009	-0.13	0.04	-0.17
7404	161.9	-72.83	26.09±0.60	0.004	0.30	0.596	0.087	0.123	0.036	-0.17	0.05	-0.22
9404	175.06	-68.40	23.28±1.13	0.005	0.00	0.745	0.286	0.330	0.044	-0.11	0.08	-0.19
16012	228.21	-56.11	34.28±0.88	0.002	-0.05	0.714	0.218	0.279	0.061	-0.14	0.10	-0.24
16738	174.32	-34.65	8.92±0.91	0.156	0.37	0.424	0.046	0.002	-0.044	0.15	0.10	+0.05
17364	260.75	-49.99	26.88±0.46	0.003	-0.11	0.515	-0.082	0.045	0.127	-0.11	0.15	-0.26
19781	179.01	-25.45	21.62±1.10	0.072	–	0.626	0.190	0.158	-0.032	-0.02	0.02	-0.04
20557	174.83	-19.05	22.59±0.77	0.051	0.12	0.469	0.001	0.015	0.014	-0.10	0.04	-0.14
21008	177.33	-19.20	21.23±0.61	0.056	0.10	0.411	-0.024	0.002	0.026	-0.01	0.06	-0.07
22449	191.45	-23.07	23.94±0.17	0.012	0.05	0.439	-0.018	0.004	0.022	0.01	0.04	-0.03
24829	257.46	-34.98	28.00±0.23	0.004	0.13	0.509	0.007	0.041	0.034	-0.01	0.03	-0.04
26617	200.92	-14.06	08.79±2.67	0.076	–	0.554	-0.025	0.080	0.105	0.16	0.13	+0.03
29248	192.32	-0.68	21.01±1.12	0.005	-0.17	0.665	0.116	0.208	0.092	0.14	0.12	+0.02
32480	172.36	17.52	59.82±0.30	0.004	–	0.550	0.055	0.076	0.021	-0.05	-0.01	-0.04
33229	265.16	-21.54	28.71±0.51	0.008	0.14	0.775	0.357	0.383	0.026	-0.11	0.06	-0.17
33277	190.42	12.06	58.00±0.41	0.002	–	0.568	0.023	0.093	0.070	0.03	0.06	-0.03
39903	274.97	-14.95	50.05±2.65	0.006	–	0.430	-0.046	0.002	0.048	0.09	0.06	+0.03
40035	234.56	10.61	44.68±0.30	0.002	-0.05	0.486	-0.021	0.025	0.046	0.03	0.03	0.00
42173	219.12	26.20	38.11±0.85	0.003	0.29	0.707	0.268	0.268	0.000	0.02	0.05	-0.03
46076	209.36	42.33	30.20±1.03	0.006	0.00	0.634	0.136	0.167	0.031	-0.05	0.04	-0.09
50473	227.30	51.40	30.90±0.68	0.007	-0.08	0.553	0.055	0.079	0.024	0.01	0.00	+0.01
51415	292.16	-11.71	16.71±0.89	0.010	-1.01	0.548	-0.107	0.074	0.181	0.16	0.27	-0.11
53818	277.02	25.40	31.86±0.36	0.009	0.37	0.515	0.026	0.045	0.019	-0.17	0.03	-0.20
54109	248.04	56.77	18.50±1.03	0.009	-0.05	0.621	0.139	0.152	0.013	0.02	0.03	-0.01
56832	260.42	62.79	28.53±0.49	0.005	0.12	0.675	0.136	0.221	0.085	-0.03	0.11	-0.14
59199	290.66	37.12	66.95±0.15	0.005	-0.04	0.327	-0.016	0.075	0.091	0.09	0.02	+0.07
66290	10.31	79.05	21.60±0.79	0.004	-0.50	0.426	-0.103	0.002	0.105	0.17	0.12	+0.05
71192	107.22	48.50	33.86±0.59	0.002	-0.29	0.488	-0.011	0.026	0.037	0.02	0.03	-0.01
73768	37.38	60.16	11.23±0.98	0.015	-0.41	0.465	-0.061	0.013	0.074	0.10	0.08	+0.02
84489	350.92	1.42	31.81±0.51	0.014	-0.15	0.465	-0.032	0.013	0.045	0.05	0.06	-0.01
86375	347.18	-6.31	17.04±0.76	0.022	–	0.699	0.229	0.256	0.027	-0.08	0.07	-0.15
92233	316.49	-26.29	24.15±0.36	0.013	0.27	0.587	0.116	0.113	-0.003	-0.13	0.02	-0.15
93827	23.95	-8.68	26.28±0.65	0.018	–	0.551	-0.045	0.077	0.122	0.03	0.17	-0.14
96507	63.27	3.58	19.89±0.56	0.015	0.18	0.570	0.154	0.095	-0.059	-0.02	0.22	-0.24
99651	27.68	-24.93	29.47±0.98	0.010	-0.63	0.703	0.133	0.262	0.129	0.09	0.17	-0.08
100925	12.18	-33.06	51.22±0.54	0.006	0.00	0.729	0.264	0.303	0.039	0.03	0.07	-0.04
107020	53.33	-37.89	24.25±0.92	0.009	-0.03	0.655	0.109	0.194	0.085	-0.14	0.11	-0.25
108456	117.67	21.84	33.44±2.53	0.015	-0.25	0.502	-0.026	0.036	0.062	0.07	0.05	+0.02
109090	83.87	-22.08	18.00±0.76	0.011	-0.23	0.519	-0.018	0.049	0.067	0.02	0.05	-0.03
113231	62.74	-56.51	27.22±1.12	0.007	–	0.633	0.081	0.166	0.085	-0.10	0.11	-0.21
118278	60.98	-76.15	39.85±0.78	0.004	0.01	0.740	0.281	0.321	0.040	-0.11	0.07	-0.18

Table 4b Data for 39 field stars taken from the same source of stars used for the calibration of the the [α/Fe] element and used for the application of the procedure. The symbols are the same as in Table 4a.

ID	l	b	π	$E_d(B-V)$	$(U-B)_0$	$(B-V)_0$	[Fe/H]	$[\alpha/Fe]_{org}$	$(U-B)_H$	δ	$[\alpha/Fe]_{cal}$	$\Delta[\alpha/Fe]$
	(^{o})	(^{o})	(mas)	(mag)	(mag)	(dex)	(dex)	(dex)	(mag)	(mag)	(dex)	(dex)
HIP 81170	11.66	27.71	22.17±1.35	0.055	0.064	0.687	-1.17	0.25	0.239	0.174	0.21	+0.04
HIP 93623	15.83	-11.82	16.37±1.47	0.012	0.039	0.641	-0.74	0.27	0.180	0.140	0.20	+0.07
HIP 80837	19.30	33.05	23.41±0.79	0.009	-0.078	0.528	-0.74	0.25	0.056	0.134	0.20	+0.05
HIP 84905	23.54	20.68	27.52±0.73	0.019	-0.029	0.560	-0.50	0.19	0.085	0.114	0.16	+0.03
HIP 86443	26.77	17.03	8.31±1.67	0.011	-0.247	0.439	-2.29	0.28	0.004	0.251	0.32	-0.04
HIP 72461	36.56	63.69	10.05±1.35	0.014	-0.239	0.411	-2.48	0.32	0.002	0.241	0.30	+0.02
HIP 83489	37.35	31.30	13.43±1.41	0.016	0.088	0.635	-0.29	0.16	0.169	0.081	0.10	+0.06
HIP 74933	39.09	57.12	12.72±1.19	0.017	-0.017	0.552	-0.39	0.04	0.078	0.095	0.11	-0.07
HIP 80003	39.52	42.85	8.16±3.37	0.028	0.058	0.675	–	0.15	0.221	0.163	0.24	-0.09
HIP 85912	42.48	25.53	26.56±0.39	0.008	-0.002	0.478	-0.23	0.09	0.020	0.022	0.03	+0.06
HIP 87693	45.55	21.25	9.38±3.43	0.022	-0.206	0.418	-2.07	0.32	0.002	0.208	0.26	+0.06
HIP 100279	49.00	-16.69	10.46±1.60	0.031	-0.070	0.583	-0.72	0.25	0.109	0.179	0.24	+0.01
HIP 97023	60.52	0.51	22.53±0.60	0.010	-0.010	0.555	-0.48	0.14	0.081	0.091	0.10	+0.04
HIP 68321	61.86	73.96	4.86±1.36	0.010	-0.216	0.389	-1.98	0.23	0.008	0.224	0.28	-0.05
HIP 78640	67.04	48.41	8.41±1.02	0.006	-0.203	0.468	-1.43	0.19	0.015	0.218	0.28	-0.09
HIP 80	82.75	-70.65	13.68±1.22	0.012	-0.089	0.538	-0.59	0.19	0.065	0.154	0.24	-0.05
HIP 113688	90.13	-36.51	12.07±0.88	0.024	0.073	0.586	-0.14	-0.01	0.112	0.039	0.05	-0.06
HIP 72407	98.57	52.33	10.65±0.73	0.003	0.071	0.617	-0.54	0.23	0.147	0.076	0.10	+0.13
HIP 74605	104.57	44.33	39.46±0.17	0.003	0.067	0.531	-0.02	0.03	0.059	-0.008	0.01	+0.02
HIP 14241	136.07	78.09	17.81±0.46	0.004	-0.023	0.476	0.04	-0.01	0.019	0.042	0.03	-0.04
HIP 57450	145.97	63.25	612.85±1.33	0.006	-0.154	0.554	-1.23	0.15	0.080	0.234	0.21	-0.06
HIP 57939	168.53	73.78	109.99±0.41	0.001	0.168	0.750	-1.27	0.20	0.338	0.170	0.27	-0.07
HIP 48113	172.78	49.43	54.44±0.28	0.001	0.143	0.612	0.04	0.06	0.141	-0.002	0.02	+0.04
HIP 14241	184.61	-51.94	28.54±0.97	0.012	0.108	0.658	-0.45	0.24	0.198	0.090	0.12	+0.12
HIP 17147	189.77	-43.12	39.12±0.56	0.007	-0.091	0.533	-0.91	0.28	0.060	0.151	0.23	+0.05
HIP 24030	195.60	-19.60	8.66±1.77	0.023	-0.147	0.497	-1.10	0.24	0.032	0.179	0.25	-0.01
HIP 19814	198.48	-37.12	13.55±2.08	0.017	0.095	0.687	-0.75	-0.03	0.239	0.143	0.18	-0.21
HIP 44033	201.91	37.86	3.97±3.04	0.022	-0.157	0.548	–	0.20	0.074	0.231	0.22	-0.02
HIP 52771	202.98	62.60	10.45±1.42	0.012	-0.233	0.488	-1.85	0.15	0.026	0.259	0.30	-0.15
HIP 61545	206.07	86.70	3.21±2.06	0.015	-0.240	0.395	-1.99	0.24	0.005	0.245	0.31	-0.07
HIP 57265	215.23	74.95	6.25±1.71	0.014	-0.147	0.465	-0.93	0.03	0.013	0.160	0.19	-0.16
HIP 44124	232.63	25.95	11.76±1.59	0.004	-0.201	0.477	-1.96	0.23	0.020	0.221	0.30	-0.07
HIP 57757	270.52	60.76	91.50±0.22	0.002	0.101	0.550	0.13	0.03	0.076	-0.025	0.05	-0.02
HIP 58843	275.45	63.66	14.24±1.33	0.008	-0.059	0.579	-0.84	0.26	0.105	0.164	0.22	+0.04
HIP 60632	288.36	63.42	9.05±1.11	0.011	-0.234	0.421	-1.75	0.23	0.002	0.236	0.30	-0.07
HIP 5054	291.21	-77.34	24.17±0.61	0.003	-0.012	0.600	-0.62	0.27	0.127	0.139	0.20	+0.07
HIP 108736	341.43	-49.37	27.95±0.55	0.004	0.569	0.565	-0.29	0.18	0.090	0.068	0.05	+0.13
HIP 92288	345.38	-20.23	11.99±1.30	0.012	0.106	0.630	-0.21	0.15	0.163	0.057	0.07	+0.08
HIP 100412	349.13	-34.67	32.24±0.47	0.005	0.551	0.546	-0.26	0.06	0.072	0.096	0.11	-0.05

Table 4c Data for 25 clusters whose $B-V$ and $U-B$ colour indices, and the colour excess $E(B-V)$, are taken from Harris (2010). While, the iron elements $[Fe/H]$ and the alpha elements [α/Fe] are provided from Dias et al. (2016).The columns give: cluster name, colour excess $E(B-V)$, $B-V$ and $U-B$ colour indices, de-reddened $(B-V)_0$ and $(U-B)_0$ colour indices, iron element [Fe/H], original alpha element $[\alpha/Fe]_{org}$, ultra-violet colour index for the Hyades cluster $(U-B)_H$, ultra-violet excess δ, estimated alpha element $[\alpha/Fe]_{cal}$, and the residual $\Delta[\alpha/Fe]$.

Cluster	$E(B-V)$	$B-V$	$U-B$	$(B-V)_0$	$(U-B)_0$	[Fe/H]	$[\alpha/Fe]_{org}$	$(U-B)_H$	δ	$[\alpha/Fe]_{cal}$	$\Delta[\alpha/Fe]$
	(mag)	(mag)	(mag)	(mag)	(mag)	(dex)	(dex)	(mag)	(mag)	(dex)	(dex)
NGC 2298	0.14	0.75	0.17	0.61	0.07	-1.95	0.19	0.14	0.07	0.09	0.097
NGC 2808	0.22	0.92	0.28	0.70	0.12	-1.06	0.24	0.26	0.14	0.18	0.062
NGC 3201	0.24	0.96	0.38	0.72	0.20	-1.51	0.22	0.29	0.08	0.12	0.096
NGC 4372	0.39	1.10	0.31	0.71	0.02	-2.20	0.21	0.27	0.25	0.27	-0.056
NGC 4590(M68)	0.05	0.63	0.04	0.58	0.00	-2.20	0.19	0.11	0.10	0.14	0.049
NGC 5694	0.09	0.69	0.08	0.60	0.01	-1.98	0.17	0.13	0.11	0.16	0.012
NGC 5634	0.05	0.67	0.09	0.62	0.05	-1.75	0.20	0.15	0.10	0.13	0.067
NGC 5824	0.13	0.75	0.12	0.62	0.03	-1.99	0.24	0.15	0.12	0.18	0.064
NGC 5897	0.09	0.74	0.08	0.65	0.01	-1.97	0.23	0.19	0.17	0.26	-0.031
NGC 5904(M5)	0.03	0.72	0.17	0.69	0.15	-1.25	0.24	0.24	0.09	0.13	0.106
NGC 5946	0.54	1.29	0.45	0.75	0.05	-1.54	0.22	0.34	0.29	0.42	-0.196
NGC 6121(M4)	0.35	1.03	0.43	0.68	0.17	-1.01	0.27	0.23	0.06	0.10	0.172
NGC 6171(M107)	0.33	1.10	0.69	0.77	0.45	-0.95	0.20	0.37	-0.07	0.01	0.185
NGC 6254(M10)	0.28	0.90	0.23	0.62	0.02	-1.56	0.21	0.15	0.13	0.18	0.032
NGC 6284	0.28	0.99	0.40	0.71	0.19	-1.07	0.27	0.27	0.08	0.12	0.151
NGC 6355	0.77	1.48	0.72	0.71	0.14	-1.46	0.27	0.27	0.14	0.18	0.094
NGC 6366	0.71	1.44	0.97	0.73	0.43	-0.61	0.30	0.30	-0.13	0.07	0.232
NGC 6397	0.18	0.73	0.12	0.55	-0.01	-2.07	0.23	0.08	0.09	0.09	0.137
NGC 6453	0.64	1.31	0.68	0.67	0.20	-1.54	0.16	0.21	0.02	0.03	0.133
NGC 6558	0.44	1.11	0.58	0.67	0.25	-1.01	0.23	0.21	-0.04	0.02	0.205
NGC 6656(M22)	0.34	0.98	0.28	0.64	0.03	-1.92	0.22	0.17	0.15	0.21	0.006
NGC 6752	0.04	0.66	0.07	0.62	0.04	-1.57	0.22	0.15	0.11	0.15	0.067
NGC 6864(M75)	0.16	0.87	0.28	0.71	0.16	-1.00	0.22	0.27	0.11	0.15	0.071
NGC 7006	0.05	0.75	0.06	0.70	0.02	-1.69	0.25	0.26	0.23	0.26	-0.006
NGC 7078(M15)	0.10	0.68	0.06	0.58	-0.01	-2.23	0.24	0.11	0.12	0.17	0.074

Table 4d Data for 19 clusters whose $B-V$ and $U-B$ colour indices are taken from Hanes & Brodie (1985). The colour excess $E(B-V)$ is taken from Harris (2010). The symbols "con." and "not" in the Remarks column indicate that the errors in $B-V$ or $U-B$ are considered or not considered, respectively. The residuals in the last column correspond to ones in Table 4c, for comparison.

Cluster	$E(B-V)$ (mag)	$B-V$ (mag)	$U-B$ (mag)	[Fe/H] (dex)	[α/Fe] (dex)	$(B-V)_0$ (mag)	$(U-B)_0$ (mag)	$(U-B)_H$ (mag)	δ (mag)	$[\alpha/Fe]_{cal}$ (dex)	$\Delta[\alpha/Fe]$ (dex)	Remarks	$\Delta[\alpha/Fe]_{4c}$ (dex)
NGC 2298	0.14	0.720±0.040	0.27±0.17	-1.95	0.19	0.62	-0.002	0.150	0.152	0.212	-0.022	con.	0.097
NGC 2808	0.22	0.900	0.18	-1.06	0.24	0.68	-0.040	0.228	0.268	0.274	-0.034	–	0.062
NGC 3201	0.24	0.980	0.45±0.09	-1.51	0.22	0.74	0.210	0.321	0.111	0.175	0.045	not	0.096
NGC 4590(M68)	0.05	0.660	0.05	-2.20	0.19	0.61	0.000	0.139	0.139	0.196	-0.006	–	0.049
NGC 5634	0.05	0.680	0.31±0.10	-1.75	0.20	0.63	0.260	0.163	-0.097	0.119	0.081	not	0.067
NGC 5694	0.09	0.690	0.01±0.05	-1.98	0.17	0.60	-0.130	0.127	0.257	0.195	-0.025	con.	0.012
NGC 5824	0.13	0.760	0.02	-1.99	0.24	0.63	-0.110	0.163	0.273	0.359	-0.119	–	0.064
NGC 5904(M5)	0.03	0.710	0.07	-1.25	0.24	0.68	0.040	0.228	0.188	0.223	0.017	–	0.106
NGC 5927	0.45	1.270	0.85±0.12	-0.21	0.30	0.82	0.280	0.469	0.189	0.301	-0.001	con.	–
NGC 5946	0.54	1.100	0.41±0.09	-1.54	0.22	0.56	-0.130	0.085	0.215	0.253	-0.033	not	–
NGC 6121(M4)	0.35	1.030	0.32±0.05	-1.01	0.27	0.68	-0.030	0.228	0.258	0.269	0.001	not	0.172
NGC 6171(M107)	0.33	1.150±0.030	0.67±0.11	-0.95	0.20	0.82	0.340	0.469	0.129	0.204	-0.004	not	0.185
NGC 6254(M10)	0.28	0.870	0.59±0.10	-1.56	0.21	0.59	0.210	0.116	-0.094	0.151	0.059	con.	0.032
NGC 6284	0.28	0.990	0.38±0.05	-1.07	0.27	0.71	0.050	0.273	0.223	0.249	0.021	con.	0.151
NGC 6355	0.77	1.500±0.030	0.62±0.11	-1.46	0.27	0.70	-0.040	0.258	0.298	0.282	-0.012	con.	0.094
NGC 6397	0.18	0.740	0.12	-2.07	0.23	0.56	-0.060	0.085	0.145	0.224	0.006	–	0.137
NGC 6441	0.47	1.300	0.79	-0.41	0.26	0.83	0.320	0.490	0.170	0.270	-0.010	–	–
NGC 6752	0.04	0.710	-0.01	-1.57	0.22	0.67	-0.050	0.214	0.264	0.357	-0.137	–	0.067
NGC 6864(M75)	0.16	0.880	0.18	-1.00	0.22	0.72	0.020	0.288	0.268	0.274	-0.054	–	0.071

Table 5a Comparison of the α elements determined in three different studies.

Star	HD108177		HD149414		BD+0203375			BD+2003603	
	Bai04	F00	Bai04	F00	Bai04	F00	S02	Bai04	F00
$[Mg/Fe]$	0.09	0.43	0.22	0.41	0.24	0.52	0.34	0.36	0.46
$[Ca/Fe]$	0.32	0.36	0.45	0.27	0.36	0.38	0.39	0.28	0.37
$[Ti/Fe]$	0.47	0.44	0.36	0.39	0.48	0.42	0.38	0.53	0.48
$[\alpha/Fe]$	0.20	0.29	0.23	0.24	0.25	0.32	0.25	0.30	0.32
Star	BD+26 2606		BD+29 2091		BD+34 2476		BD+42 2667		
	Bai04	F00	Bai04	F00	Bai04	S02	Bai04	F00	S02
$[Mg/Fe]$	0.25	0.42	0.11	0.38	0.17	0.27	0.09	0.41	0.36
$[Ca/Fe]$	0.28	0.37	0.24	0.42	0.34	0.49	0.32	0.38	0.33
$[Ti/Fe]$	0.63	0.52	0.38	0.54	0.43	0.44	0.39	0.36	0.31
$[\alpha/Fe]$	0.30	0.32	0.13	0.33	0.20	0.29	0.16	0.26	0.21

(1) Bai04: Bai et al. (2004), (2) F00: Fulbright (2000), (3) S02: Stephens & Boesgaard (2002).

Table 5b Comparison of the δ elements determined in different studies.

Star	[α/Fe]		Star	[α/Fe]	
	V04	B14		V04	N10
HIP 47048	0.06	0.14	HIP 19797	0.30	0.20
HIP 107975	0.18	0.11	HIP 57265	0.13	0.03
HIP 60632	0.34	0.25	HIP 94449	0.33	0.26
HIP 72673	0.19	0.14	HIP 24030	0.27	0.24
HIP 110341	0.09	0.04	HIP 58229	0.13	0.09
HIP 3026	0.23	0.15	HIP 7459	0.10	0.15
HIP 2711	-0.05	0.06	HIP 36818	-0.03	0.04
HIP 78640	0.30	0.27	–	–	–
HIP 9085	0.07	0.07		V04	R06
HIP 22632	0.19	0.25	HIP 88039	0.30	0.24
HIP 699	0.16	0.05	HIP 52771	0.36	0.11
HIP 910	0.09	0.08	HIP 31188	0.14	0.05
HIP 96536	0.07	0.00	HIP 99938	0.30	0.16
HIP 58145	0.18	0.26	HIP 10449	0.27	0.14
HIP 3909	0.06	-0.02	HIP 85373	0.25	0.10
HIP 22325	0.08	-0.01	HIP 85378	0.30	0.24
HIP 16404	0.37	0.17	HIP 25860	0.25	0.18
HIP 67863	0.20	0.27	–	–	–
HIP 5054	0.22	0.27	–	–	–
HIP 7276	0.07	-0.01	–	–	–

Note: V04: Venn et al. (2004), B14: Bensby et al. (2014), N10: Nissen & Schuster (2010), R06: Reddy et al. (2006).

Table 6 Percentages of the stars (%) with (absolute) residuals less than 0.15 and 0.20 in four panels of Fig. 5.

Panel $\rightarrow$	(a)	(b)	(c)	(d)
$\lvert\Delta$[Fe/H]$\rvert < 0.15$	63	92	80	100
$\lvert\Delta$[Fe/H]$\rvert < 0.20$	79	100	92	100